

polymer papers

Reactive compatibilisation of A/(B/C) polymer blends

Part 1. Investigation of the phase morphology development and stabilisation

K. Dedecker and G. Groeninckx*

Katholieke Universiteit Leuven, Department of Chemistry, Laboratory for Macromolecular Structural Chemistry, Celestijnenlaan 200 F, 3001 Heverlee, Belgium (Accepted 2 September 1997)

The compatibilisation of immiscible blends of polyamide 6 (PA-6) and poly(methyl-methacrylate) (PMMA) using a reactive copolymer styrene–maleic anhydride (SMA) has been investigated. In a first series of experiments, SMA20 (20 wt% MA) was used as the reactive copolymer, and this compatibilisation method turned out to be quite efficient. Five to 6 wt% SMA20 copolymer was needed to obtain the minimum particle size for the dispersed PMMA-phase in the blend PA-6/PMMA (75/25). From melt-blending experiments during which the phase morphology was analyzed as a function of the extrusion time, it was concluded that the diffusion of SMA towards the PA-6/PMMA interface is the rate limiting step for the formation of the graft copolymer PA-6-g-SMA and as a consequence for the reactive compatibilisation process. By varying the percentage dispersed phase of the blends, it was possible to examine the role of coalescence with respect to the size of the dispersed particles. It was concluded that the reduction of coalescence in the compatibilised blends is the main reason for the dispersed phase particle size reduction. The miscibility between PMMA and SMA copolymers with a varying MA content ranging from 10 up to 35 wt% MA offers a unique opportunity to study the effect of the degree of functionality of the reactive copolymer on the compatibilisation process. The use of SMA copolymers with a different MA content revealed that the functionality of SMA is a very critical parameter with respect to its compatibilising efficiency in the blends because it influences the miscibility of SMA with PMMA. Finally, experiments with low-molecular weight PA-6 revealed that the added SMA compatibiliser is more efficiently used in this case. © 1998 Elsevier Science Ltd. All rights reserved.

(Keywords: reactive compatibilisation; interfacial modifier; particle size reduction)

INTRODUCTION

The development of new multiphase polymeric materials often involves the blending of two or more polymers. The combination of the favourable properties of different polymers is most likely the goal of blending. Due to the low combinatorial entropy of mixing, most binary polymer blends are immiscible giving rise to a two-phase system which is mostly characterised by a coarse and unstable phase morphology and a poor interfacial adhesion between the phases. These problems can be solved by means of compatibilisation, which consists in the modification of the interfacial properties of the blend phases. This method is most often based on the use of suitable block or graft copolymers which are located at the interface between the phases of an immiscible blend and act as an emulsifying agent.

In the past, much attention has been paid to the synthesis of block and graft copolymers as potential compatibilisers, which were subsequently added to an immiscible blend¹. However, this strategy can not be applied for all kinds of blends and, moreover, the synthesis is most often very expensive. For these reasons, most of the interest is now going to a method called 'reactive' compatibilisation; it is based on the in situ formation of a block or graft copolymer

at the interface between the phases as a result of chemical reactions during melt-mixing².

In most cases, the two components of a binary blend do not have the appropriate reactive groups for the formation of a copolymer at the interface and, as a consequence, functionalisation is required. Functionalisation of the blend components is a widely applied strategy for reactive compatibilisation. In recent years, research has been performed to realise functionalisation of different types of polymers, and to obtain a good insight into the reactivity of different functional groups to obtain the desired compatibilisation effect².

Another method of reactive compatibilisation is based on the addition of a reactive polymer to the blend as a third component. It is necessary that this reactive polymer is miscible with one of the blend components and reactive with the other blend component. A reactive polymer which fulfils these conditions can only be found for a limited number of binary blends (*Figure 1*). Most of the studies related to this method of reactive compatibilisation are based on the miscibility of the reactive copolymer styrene–maleic anhydride (SMA) with styrene–acrylonitrile copolymer (SAN) under well-defined copolymer compositions³.

This paper also deals with this method of in situ reactive compatibilisation. The copolymer SMA is miscible with poly(methyl-methacrylate) (PMMA) depending on its

* To whom correspondence should be addressed.

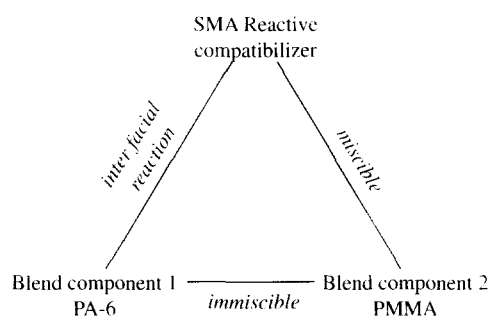


Figure 1 Schematic representation of the strategy of compatibilisation used for PA-6/PMMA blends

degree of functionality (MA content of SMA). On the other hand, the anhydride groups of SMA can react with the amino end groups of polyamide 6 (PA-6) which leads to the formation of a comb-like graft copolymer at the interface due to the interfacial imidisation reactions⁴⁻⁶.

In this paper, the efficiency of the proposed compatibilisation method has been investigated for the blend system PA-6/PMMA. The phase morphology of this blend has been examined as a function of material parameters such as the amount of compatibiliser (% SMA), type of compatibiliser (% MA in SMA), amount of dispersed phase, molecular weight of the components, as well as a function of mixing parameters such as mixing time and screw rotation speed. The blend phase morphology is interpreted in terms of necessary extrusion time (diffusion time + reaction time) for the formation of the graft copolymer, compatibilising efficiency and interfacial stability of the formed graft copolymer. The reason for the particle size reduction in the compatibilised blends is also discussed. The system PA-6/(PMMA/SMA) offers the opportunity to study the use of reactive compatibilisers with a high amount of reactive groups. Furthermore, the miscibility of PMMA with a lot of different SMA types with an MA content from 10 up to 35 wt% makes it possible to use reactive polymers with a varying amount of functional groups.

This work can be considered as a model study in which some of the principles and concepts which have been applied, are also valid for other reactively compatibilised blend systems.

EXPERIMENTAL

Materials

The characteristics of the blend components are given in Table 1. Four different types of PA-6 were used; they were all provided by DSM-Research. PMMA was provided by Rohm and Haas under the commercial name DIAKON MG-102. SMA17, SMA20, SMA25 and SMA33 were supplied by BAYER; SMA14 and SMA28 were provided by Arco. The number after SMA denotes the wt% maleic anhydride in SMA. The molecular weight of the polymers were determined using gel permeation chromatography (GPC) and intrinsic viscosity measurements.

Blend preparation

The blends were prepared in a double-screw mini-extruder designed by DSM-Research (The Netherlands). It consists of a mixing chamber with a capacity of 4 g and two corotating conical screws. By means of a recirculation channel within the mixing chamber and a valve to open the

Table 1 The characteristics of the different blend components

Material	Method	M_w
PA6	[η] in HCOOH/H ₂ O 85/15 at 25°C	18 000
PA6		24 000
PA6		35 000
PA6		44 000
PMMA	GPC in THF [η] in THF at 25°C	69 000
SMA14		190 000
SMA17		210 000
SMA20		125 000
SMA25		220 000
SMA28		130 000
SMA33		90 000

mixing chamber, the residence time can be varied. The mixing chamber can be saturated with nitrogen gas during melt-blending to avoid oxidative degradation of the blend components PA-6 and PMMA^{7,8}. The extrusion temperature was always kept constant at 240°C during blending and the screw speed was 100 rpm, unless otherwise noted.

The blend components PMMA and SMA were premixed during 3 min in order to obtain a miscible blend. PA-6 is subsequently added to this premixed PMMA/SMA blend. The mixing time is recorded from the moment all the PA-6 is added. This mixing procedure was compared to the method in which the three components were simultaneously added⁹⁻¹¹. A comparison of the phase morphology revealed no essential differences between these two mixing procedures. However, the procedure in which PMMA and SMA are premixed, was used in further experiments.

After blending, the extruded polymer strand was quenched in a mixture of isopropanol/CO₂ (-78°C) in order to freeze in the phase morphology. In all blends studied, PA-6 forms the matrix while the dispersed phase consists of the miscible components PMMA and SMA. All blends consist of 75 wt% PA-6 ($M_w = 44\,000$) and 25 wt% PMMA + SMA, unless otherwise noted.

Characterisation of the blends

The extruded polymer strands were held in liquid N₂ for some time and a brittle fracture was performed. This brittle surface was etched with chloroform during 48 h at room temperature in order to dissolve the dispersed phase (PMMA + SMA). The etched surface was kept under vacuum before coating it with a gold layer of ± 40 nm. After gold coating, the morphology was examined with a Phillips XL-20 scanning electron microscope¹².

For each blend, different micrographs with a total amount of ± 600 particles were made. These micrographs were analyzed with a camera and the diameter of each particle was calculated¹³. A number average diameter (D_n) and a weight average diameter (D_w) were calculated according to the following formula:

$$D_n = \frac{\sum N_i D_i}{\sum N_i} \quad (1)$$

$$D_w = \frac{\sum N_i \cdot D_i^2}{\sum N_i D_i} \quad (2)$$

The interfacial area (A_{3D}) per volume unit of the dispersed phase (V_{3D}) was calculated from the total perimeter of the particles (P_{2D}) divided by the total area of the particles

(A_{2D}), as obtained from the micrographs:

$$A_i (\mu\text{m}^2/\mu\text{m}^3) = \frac{P_{2D} (\mu\text{m})}{A_{2D} (\mu\text{m}^2)} = \frac{A_{3D} (\mu\text{m}^2)}{V_{3D} (\mu\text{m}^3)} \quad (3)$$

RESULTS AND DISCUSSION

Blend phase morphology development versus extrusion time

It is generally accepted that the in situ formation of a graft copolymer at the interface between the phases in a blend leads to a finer phase dispersion. A relevant parameter is the extrusion time necessary to complete this reaction and to obtain a morphology which is invariant with further increasing extrusion time. This parameter was investigated as a function of the percentage added SMA20.

For the blend PA-6/(PMMA/SMA20) with a weight ratio 75/(24/1), the refinement of the phase morphology is a very slow process, as can be seen from *Figure 2*; almost 30 min were required to obtain a final morphology. During the development of the morphology as a function of the blending time, besides many small dispersed particles, also larger particles were present which exhibited a complex shape and tended to form a co-continuous morphology. This complex, co-continuous morphology could only be quantified after ultramicrotomy (*Figure 3*). In *Figure 2*, the ordinate is the interfacial area per volume unit of dispersed phase. This parameter is used here instead of the weight average particle diameter because of the co-continuity of the blends. After a blending time of about 30 min, this co-continuous morphology disappeared and finally the morphology consisted of a particle dispersion in a matrix.

For the blend PA-6/(PMMA/SMA20) with weight ratio 75/(23/2), a long extrusion time is also required to obtain a final morphology. Again, the phases have initially a complex and co-continuous shape, and finally a dispersion in a matrix is observed. However, as the amount of SMA20 in the blend is further increased, the necessary extrusion time to obtain an equilibrium morphology is drastically decreased. For blends with minimum 3 wt% SMA20, an extrusion time of 3 min is sufficient to obtain an equilibrium morphology.

For each of the blends studied, the weight average particle diameter (or the amount of interfacial area) was measured as a function of the extrusion time. In this way, the necessary extrusion time to obtain an equilibrium morphology was

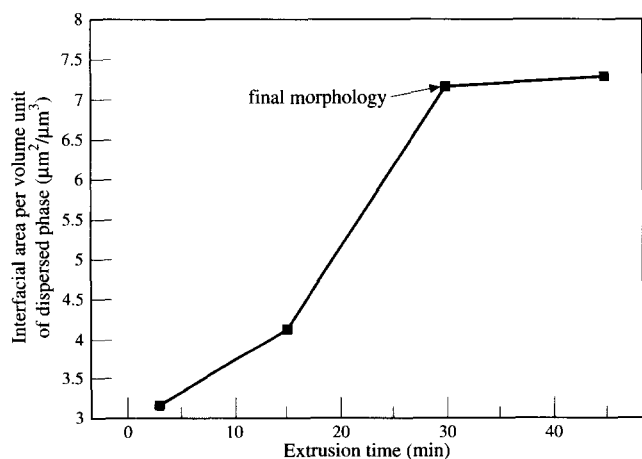


Figure 2 The interfacial area per volume unit dispersed phase versus the extrusion time for the blend PA-6/(PMMA/SMA20) 75/(24/1)

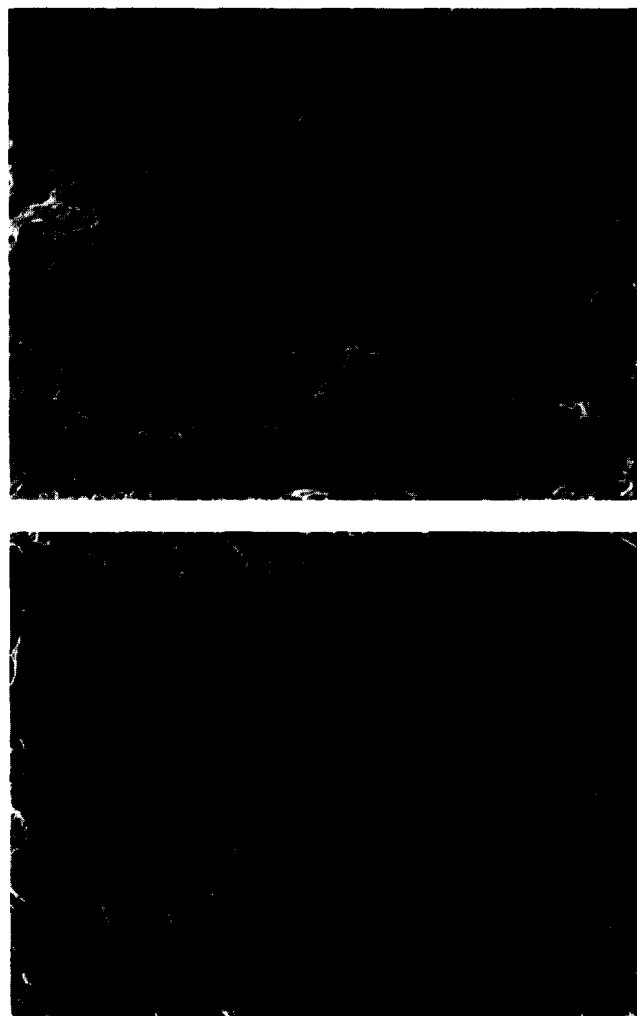


Figure 3 Morphology of the blend PA-6/(PMMA/SMA20) 75/(24/1) (extrusion time = 15 min) (a) before ultramicrotomy (b) after ultramicrotomy

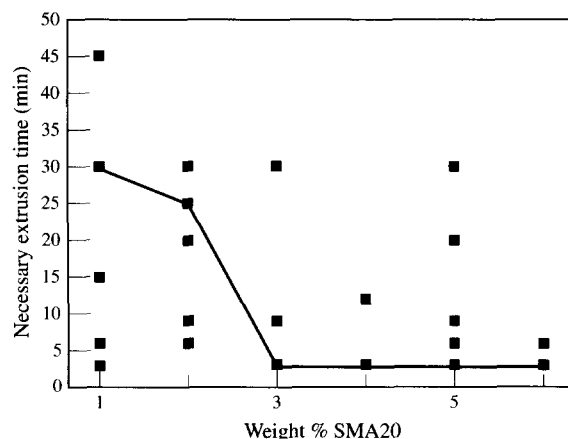


Figure 4 The necessary extrusion time to obtain an equilibrium morphology as a function of the SMA20 content in the blend PA-6/(PMMA/SMA20) 75/(25-x/x)

determined. The necessary extrusion time as a function of the SMA20-content is given in *Figure 4*. The points below the indicated line represent morphologies which are still in development; those above the line and on the line represent equilibrium morphologies.

The trend presented in *Figure 4* can be interpreted as follows. When low contents of SMA20 are added (f.e. 1 wt%), the amount of interfacial area will initially be relatively low (*Figure 2*). Only a very limited amount of SMA20 will be close enough to the PA-6/PMMA interface to react immediately. The remaining amount of SMA20 will have to diffuse over large distances, which will take a longer time. When larger amounts of SMA20 are added (f.e. 5%), the amount of SMA20 which can immediately react will be higher. The reaction of this SMA20 can already cause a significant particle size reduction (similar increase in interfacial area). In these smaller particles, the diffusion distance of the remaining SMA20 towards the interface is decreased and the amount of interfacial area is increased. In this way, the formation of the equilibrium morphology will be very fast. It is important to note that the very fast formation of the equilibrium morphology in blends with minimum 3 wt% SMA20 is only possible because of the particle size reduction during extrusion.

It is also clear that the particle size in the non-compatibilised blends will determine the initial diffusion distance of SMA20 towards the interface and the initial amount of reaction area. In this way, parameters such as the viscosity ratio, screw rotational speed, interfacial tension and amount of dispersed phase which influence the particle size in the non-compatibilised blends, will also affect indirectly the interfacial reaction rate. The following experiment was set up to test the effect of the screw rotational speed on the morphology development. The blend PA-6/(PMMA/SMA20) with a weight ratio 75/(24/1) was prepared at a screw speed of 15 rpm (instead of 100 rpm). After an extrusion time of 30 min, the interfacial area per volume unit of the dispersed phase is only $3.41 \mu\text{m}^2/\mu\text{m}^3$ and the typical developing phase morphology (as observed for all the points under the line in *Figure 4*) is observed.

The equilibrium morphologies which were obtained will now be compared to each other. The weight average diameter of the dispersed particles is presented in *Figure 5* as a function of the SMA20 content in the blend. Some SEM micrographs are given in *Figure 6*. As can be seen, low amounts of SMA20 (2–3 wt%) cause the greatest particle size reduction. This is an important factor with respect to the acceleration of the graft copolymer formation at the interface during melt-mixing as discussed in the last paragraph. The particle size reaches a minimum value ($\sim 0.15 \mu\text{m}$) at 5–6 wt% SMA20.

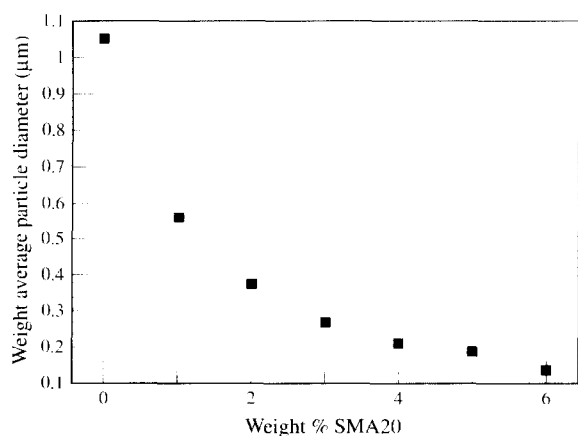


Figure 5 The weight average particle diameter as a function of the SMA20 content in the blend PA-6/(PMMA/SMA20) 75/(25-x/x)

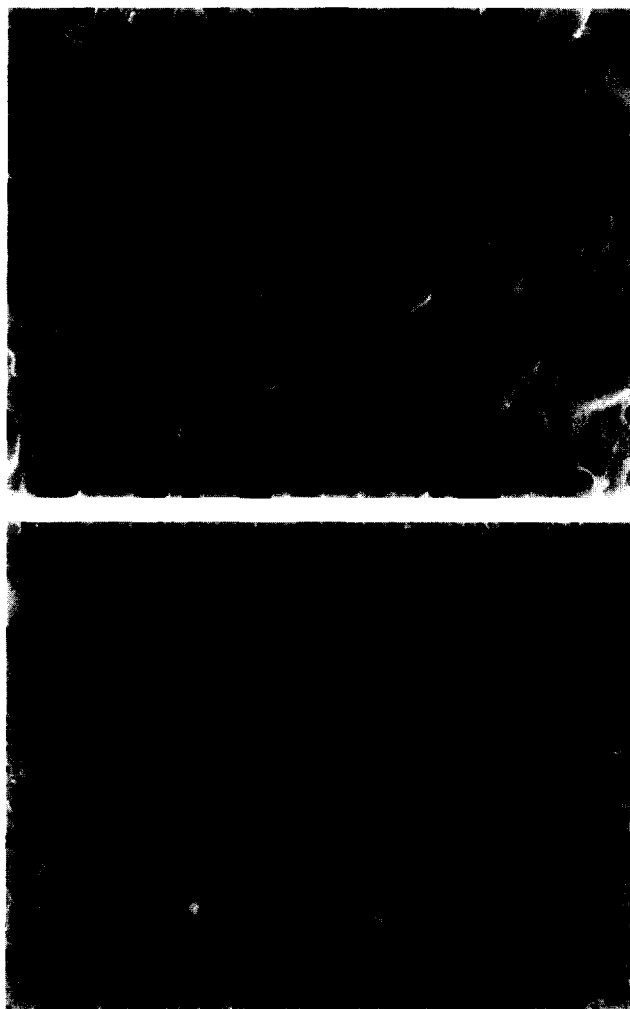


Figure 6 SEM micrographs of the blend PA-6/(PMMA/SMA20) (A) 75/(25/0); (B) 75/(19/6)

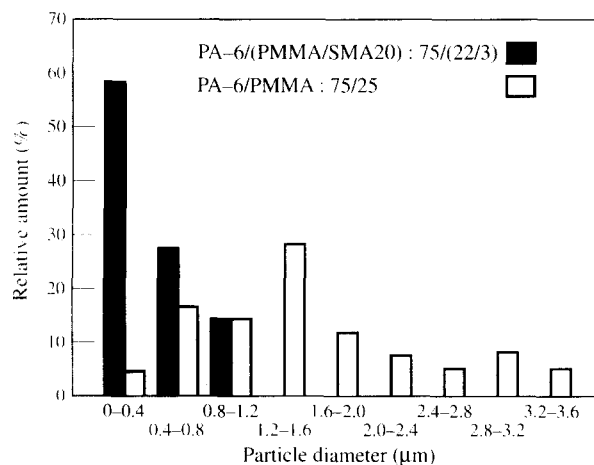


Figure 7 The particle size distribution (weight average) in a compatibilised and a noncompatibilised PA-6/PMMA blend

It was observed that the dispersed particles showed a more spherical shape and a more uniform size as the amount of added SMA20 was increased. The relative number of particles in a stage of break-up also decreased with the addition of SMA20. As can be seen from *Figure 7*, the polydispersity in particle size also decreased with the

addition of SMA20. This clearly reflects the reduced rate in coalescence as the particles become covalently bonded to the matrix. Coalescence tends to broaden the particle size distribution. The role of coalescence in polymer blends has recently been studied more fundamentally by Fortelny *et al.*^{14,15}. The role of the coalescence process with respect to the final particle size in our study will be discussed in more detail in the next section.

Particle size reduction of the dispersed phase: coalescence versus interfacial tension

Many papers^{16–18} in the past have ascribed the observed particle size reduction of the dispersed phase in compatibilised blends to a decrease of the interfacial tension. Recently, it was suggested that the reduction of coalescence in compatibilised blends might also play a crucial role with respect to the particle size reduction¹⁹. The role of coalescence can be estimated by varying the amount of dispersed phase since the probability of collision is related to it²⁰. The experiments were performed for blends without compatibiliser, as well as for two blends with a different amount of compatibiliser. The weight average particle diameter is given in *Figure 8*. As expected, the rate of coalescence is quite high for blends without compatibiliser. For blends with an intermediate amount of compatibiliser (PMMA/SMA20 = 22/3), coalescence is almost completely suppressed. For the blends with a higher amount of compatibiliser (PMMA/SMA20 19/6), coalescence is completely absent; for these blends, the particle size is independent of the amount of dispersed phase. The reduced rate of coalescence in compatibilised blends is interpreted as being due to the increased steric hindrance at the interface as the dispersed particles become covalently bonded to the matrix. The mobility of the interface is a critical parameter for the coalescence of two dispersed particles²⁰.

In *Figure 8*, it can also be seen that for blends with 1 wt% dispersed phase, the particle size is almost independent of the composition of the dispersed phase (with or without compatibiliser). For these blends with 1 wt% dispersed phase, the rate of coalescence is extremely low for the three types of blends, because the probability for collisions is almost zero^{21,22}. These data indicate that the decrease in interfacial tension in the compatibilised blends under consideration does not give rise to a particle size reduction. When a reduced rate of coalescence is considered to explain the effect of compatibilisation on the particle size, the

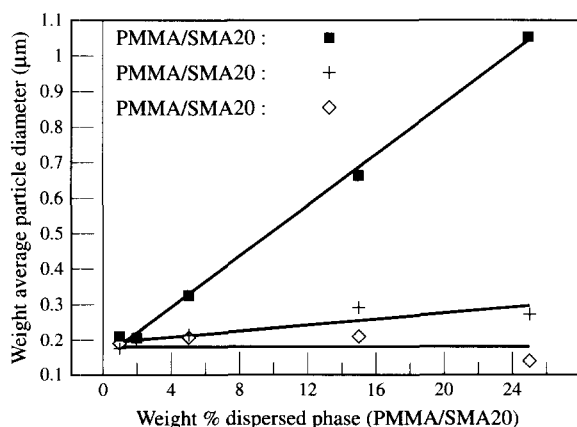


Figure 8 The weight average particle diameter as a function of the weight percent dispersed phase in PA-6/(PMMA/SMA20) blends. The composition of the dispersed phase is indicated

particle size data obtained at 1 wt% dispersed phase and at 25 wt% dispersed phase can easily be interpreted.

The coalescence process between dispersed particles was further investigated in a model coalescence experiment. In this model experiment, two populations of particles were mixed together for 20 min in the mini-extruder under normal operating conditions. One population consisted of particles with a composition of PMMA/SMA20 19/6 in a matrix of PA-6. These particles are unable to coalesce and are considered to have an immobile interface. The second population consisted of PMMA particles in a PA-6 matrix. These particles are considered to have a mobile interface and a high rate of coalescence. The important aspect in this model experiment was to investigate the ability of the two populations to coalesce. If this is the case, then a new intermediate population has to be expected; if coalescence is impossible, then a bimodal population has to be observed. An intermediate population was observed indicating that two immobile interfaces are required to prevent particles to coalesce.

Optimum functionality of the SMA compatibiliser

For the previous blends studied, SMA20 has been used as a reactive compatibiliser. SMA compatibilisers with other MA contents have also been used. Their characteristics are given in *Table 1*. With respect to their compatibilising efficiency, it is very important to take into account the miscibility behaviour between SMA and PMMA. This was investigated by Paul and co-workers^{23,24}; PMMA/SMA blends always show an LCST behaviour. At the extrusion temperature of 240°C, SMA is miscible with PMMA for MA contents between ± 10 and 35%. As the cloud point of the PMMA/SMA blends depends on the molecular weight of PMMA and SMA and on the blend composition, the miscibility behaviour was checked for the components used.

The compatibilised blends PA-6/(PMMA/SMA) under consideration have the composition 75/(20/5). The miscibility behaviour was thus analyzed for the PMMA/SMA blends in a weight ratio 80/20; they were prepared at 240°C in a mini-extruder. The transparency of the blends was considered as a first indication of miscibility. The blends of PMMA with SMA14, SMA17, SMA20, SMA25 and SMA28 were transparent after 3 min extrusion. The blend PMMA/SMA33 (80/20) was opaque at short extrusion times but became transparent after longer extrusion times (~ 10 min). Due to the higher T_g of SMA33 and the weak miscibility of SMA33 with PMMA, the interdiffusion is probably slower. The blend PMMA/SMA8 remained opaque, even after longer extrusion times (~ 10 min) indicating that this blend is not miscible at 240°C. The blends PMMA/SMA were annealed at different temperatures for 2 min and then quenched in liquid nitrogen. The miscibility was evaluated using differential scanning calorimetry; the blends with one T_g were considered as miscible while the blends with two T_g values were considered as immiscible. When the T_g values were too close to each other to judge whether one or two T_g values were present, the blends were annealed under T_g to obtain an exothermic peak (enthalpy relaxation)²⁵. The results of the d.s.c. measurements are given in *Figure 9*.

The weight average particle diameter has been evaluated as a function of the extrusion time for the blend PA-6/(PMMA/SMA) with a weight ratio 75/(20/5) with three different compatibilisers (SMA20, SMA28 and SMA33). The results are presented in *Figure 10*. Compared to the particle size data obtained with SMA20, a complete

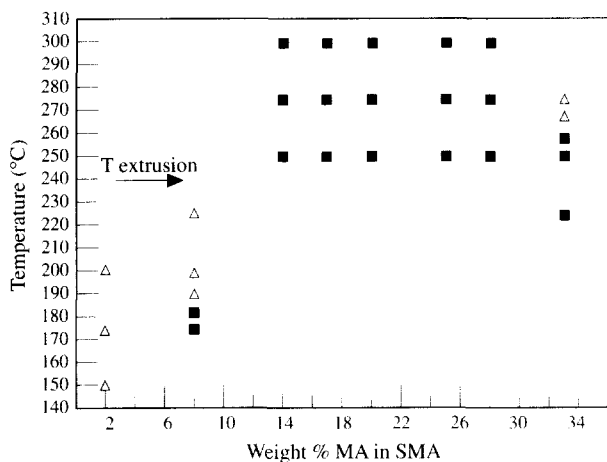


Figure 9 The miscibility of blends PMMA/SMA 80/20 as a function of the MA content in SMA. (■) miscible; (△) immiscible

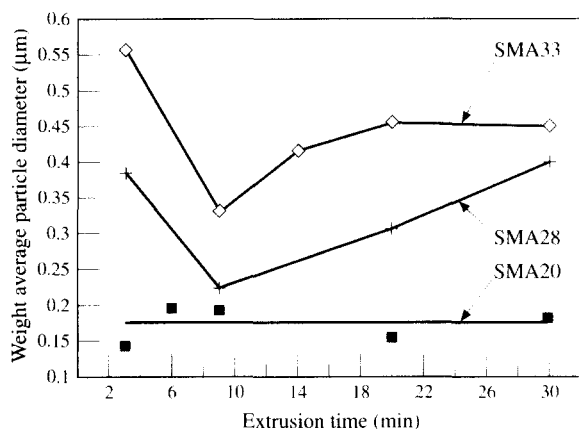


Figure 10 The weight average particle diameter as a function of the extrusion time for the blend PA-6/(PMMA/SMA) 75/(20/5)

different behaviour is observed with SMA28 and SMA33 as compatibilisers. The particle size can still decrease after 3 min of extrusion for blends with 5% SMA28 and 5% SMA33, while this was not the case for blends with 5% SMA20. There are several factors which can explain this slower formation of the minimum particle size for SMA28 and SMA33. Firstly, it should be mentioned that the premixing between PMMA and SMA will be less efficient as SMA has a higher T_g and is thermodynamically less miscible with PMMA. This can cause part of the SMA not to be well mixed with PMMA and not to act as a compatibiliser. As already discussed, the lower the amount of compatibiliser, the longer the necessary time required to obtain an equilibrium particle size. Secondly, the rate of diffusion of the compatibiliser towards the interface may be different for different SMA types. The rate of diffusion of SMA towards the interface depends on the T_g of the dispersed phase, the molecular weight of PMMA and SMA and also on the thermodynamic miscibility between SMA and PMMA²⁶.

A new observation, as can be seen from Figure 10, is the increase of the average particle size at long extrusion times for blends with 5% SMA28 and 5% SMA33. This increase was not present for the blends with 5% SMA20. As already suggested by other authors^{27,28}, the formed graft copolymer

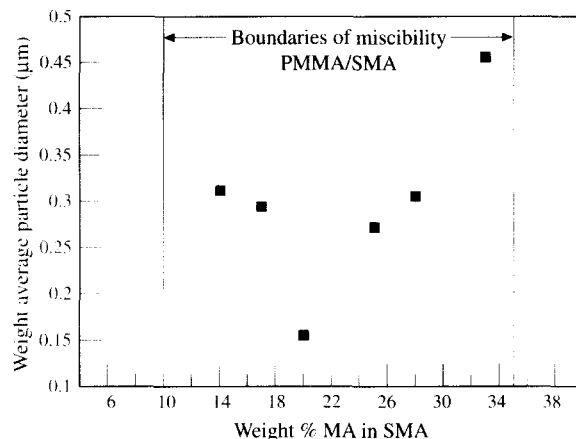


Figure 11 The weight average particle diameter of the blend PA-6/(PMMA/SMA) 75/(20/5) as a function of the MA content in SMA. All the blends contain 5% SMA and were extruded at 240°C for 20 min

probably slowly leaves the interface; this might be due to mechanical forces exerted by the screws of the extruder on the polyamide side chains of the graft copolymer. It was observed that this increase in particle size was fastened when the screw speed was increased from 100 up to 250 rpm during extrusion. It was also observed that the particle size increase of the blends was accompanied by a pronounced increase in blend viscosity. It is suggested that the graft copolymer diffuses into the PA-6 matrix and forms very small, highly grafted micelles in the polyamide matrix which could explain the increase in viscosity^{29,30}.

The weight average particle size has been analyzed after an extrusion time of 20 min for the blend PA-6/(PMMA/SMA) in a weight ratio 75/(20/5) for SMA compatibilisers having a different MA content. This is shown in Figure 11. For the compatibilisers close to the boundaries of the miscibility region of PMMA and SMA, a large particle size of the dispersed phase is observed after a long extrusion time. The increase in particle size of the dispersed phase seems to be correlated with the degree of miscibility between SMA and PMMA. It is considered that the degree of miscibility of the SMA main chain sequences of the graft copolymer with the dispersed PMMA phase acts as a thermodynamic force against the mechanical force exerted by the extruder screws on the PA-6 side chains of the graft copolymer.

The very complex chain structure of the formed graft copolymer, due to the high functionality of the compatibiliser (such as SMA20), is often used to explain its difficult location at the interface³¹. By our experiments it is now proven that a weak miscibility of the main chain of the graft copolymer is rather the limiting factor for a stable location at the interface. It is also important to note that the miscibility of the grafted SMA with PMMA will be modified by the reaction. The number of anhydride groups is decreased and newly formed imide groups are present. Both factors are expected to influence the miscibility of grafted SMA with PMMA in the interfacial region.

Molecular weight effect of the matrix polymer

In the blends studied, the molecular weight of the PA-6 matrix was always 44 000. Another PA-6 with a lower molecular weight has also been used (see Table 1). The comparison between a low-molecular weight (LMW; $M_w = 18\ 000$) and a high-molecular weight (HMW; $M_w = 44\ 000$)

PA-6 matrix is presented in Figure 12. The weight average particle size is given as a function of the amount of SMA. In the non-compatible blends, the dispersed particles are much larger in the case of the LMW matrix. However, this difference disappears completely as 1% SMA20 is added; the particle size in a LMW matrix is comparable to that in a HMW matrix. From 2% SMA20 on, the particles are smaller for the LMW matrix. These trends are confirmed for different molecular weights of the matrix in Figures 13 and 14.

The larger particles observed in the non-compatible blends with a LMW matrix can easily be explained according to the equation of Fortelny *et al.*¹⁴. The first term of equation (4) reveals the minimum obtainable particle size according to the classical theory of break-up; the second term represents the coalescence effect.

$$R = \frac{\sigma_{12} \cdot (We)_c}{\eta_m \cdot \gamma} \cdot \frac{\sigma_{12} \cdot \alpha}{\eta_m \cdot f_1} \cdot \phi \quad (4)$$

In this equation, $(We)_c$ represents the critical Weber number, η_m the viscosity of the matrix (Pa·s), σ_{12} the interfacial tension (N/m), γ the shear rate (s^{-1}), R the particle size, α the probability of coalescence after collision, ϕ the volume fraction of the dispersed phase and f_1 the slope of the function $F(We)$, describing the frequency of breakups of droplets at the critical Weber number $(We)_c$. By lowering the molecular weight of the matrix, its viscosity is also lowered. In this way, the dispersive forces for particle

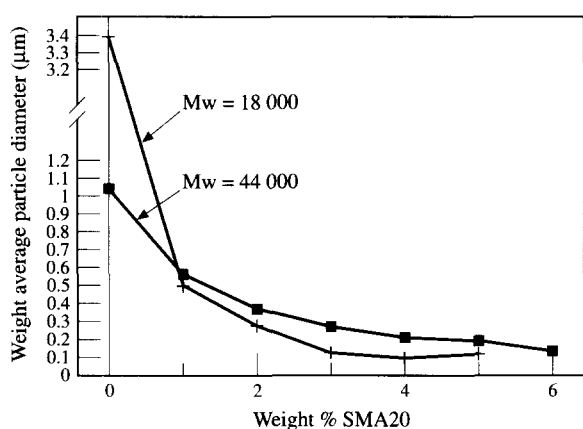


Figure 12 The weight average particle diameter as a function of the SMA20 content in the blend PA-6/(PMMA/SMA20) 75/(25-x/x) for two different molecular weights of PA-6

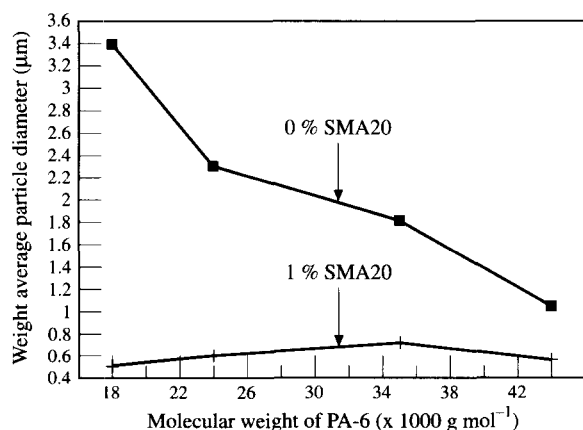


Figure 13 The weight average particle diameter as a function of the molecular weight of the PA-6 matrix for blends PA-6/(PMMA/SMA20) 75/(25-x/x) without and with 1% SMA20

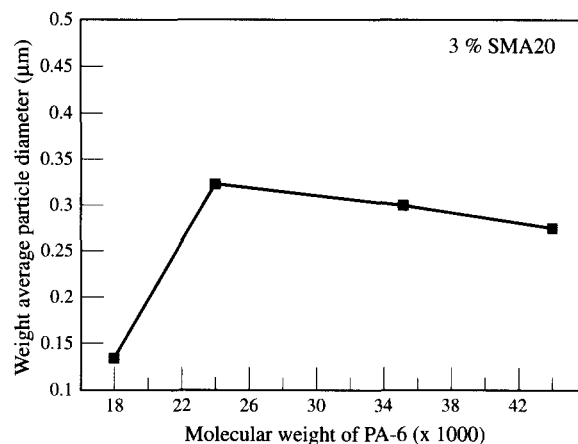


Figure 14 The weight average particle diameter as a function of the molecular weight of the PA-6 matrix for blends PA-6/(PMMA/SMA20) 75/(25-x/x) with 3% SMA20

break-up are lowered on the one hand and coalescence is enhanced on the other hand. These two parameters represent the two factors η_m in the denominator of equation (4). Lowering the matrix viscosity will also influence the critical Weber number $(We)_c$ because it is a function of the viscosity ratio η_d/η_m . $(We)_c$ reaches its minimum value when the viscosity ratio η_d/η_m is 1. The viscosity of the different polymers was measured with a capillary rheometer. The method is described in Part 2 of this series of papers³². It was found that the viscosity ratio is close to 1 for the HMW PA-6 matrix and higher than unity for the LMW PA-6 matrix. These data also support the existence of larger dispersed particles in a LMW PA-6 matrix.

The very small dispersed particles observed in compatible blends with a LMW PA-6 matrix and the faster decrease in particle size with the addition of SMA20 indicates that the added SMA20 is more efficiently used. It is, however, not easy to explain these phenomena. The following factors have to be taken into account:

(1) The number of reactive amino endgroups is higher for the LMW PA-6. However, it is proven in Part 3 that the use of a low molecular weight PA-6 does not lead to a higher degree of grafting in the comparable blend system PA-6/(PS/SMA2).

(2) In the blend system PA-6/(PS/SMA2), the formed graft copolymer leaves the interface in order to form micelles within the PA-6 matrix (Part 3). In this particular system, this effect is observed for the HMW PA-6 but not for the LMW PA-6, and results in a larger particle size in blends with a HMW PA-6 matrix compared to the LMW PA-6 matrix.

The influence of the molecular weight of PA-6 is discussed in more detail in Part 3³³, where the relation between particle size, extent of reaction and interfacial thickness is discussed.

CONCLUSIONS

In Part 1 of this series of papers, the different parameters influencing the efficiency of compatibilisation of PA-6/PMMA blends with SMA were evaluated. The main conclusions are as follows.

(1) The diffusion of SMA in the PMMA phase towards the interface is the rate-limiting step for the formation of the graft copolymer. During melt-mixing, the interfacial grafting reaction leads to smaller dispersed particles, and hence

also to a shorter diffusion distance of SMA towards the interface. The interfacial reaction accelerates itself in this way.

(2) The main reason for the particle size reduction in the compatibilised blends is a reduced rate of coalescence which is due to an immobile interface. The role of the interfacial tension with respect to the particle size reduction is very limited.

(3) It was stated that the mechanical stress exerted by the screws on the polyamide side chains of the graft copolymer (PA-6-g-SMA) tends to remove the graft copolymer from the interface and to coarsen the morphology at long extrusion times. This is counteracted by thermodynamic forces resulting from the miscibility of the SMA main chain sequences with PMMA. The miscibility of the reactive SMA compatibiliser with the PMMA phase determines the phase stability in the blend at long extrusion times.

(4) The use of a low-molecular weight PA-6 matrix leads to relatively large dispersed particles in the non-compatibilised blends. This can be accounted for by a less efficient break-up and a higher rate of coalescence. This low-molecular weight matrix, however, produces very small compatibilised particles. The added SMA20 is more efficiently used.

ACKNOWLEDGEMENTS

The financial support of the Research Council KU Leuven and the Fund for Scientific Research–Flanders (FWO–Vlaanderen) is gratefully acknowledged. The authors are also indebted to the Flemish Institute I.W.T. for a Ph.D. research grant to one of them (K.D.).

REFERENCES

- Fayt, R., Jérôme, R. and Teyssié, Ph., *Polym. Eng. Sci.*, 1987, **27**, 328.
- Xanthos, M., *Polym. Eng. Sci.*, 1988, **28**, 1392.
- Triacca, V. J., Ziaee, S., Barlow, J. W., Keskkula, H. and Paul, D. R., *Polymer*, 1991, **32**, 1401.
- Scott, C. and Macosko, C., *J. Polym. Sci.: Part B: Polym. Phys.*, 1994, **32**, 205.
- Ide, F. and Hasegawa, A., *J. Appl. Polym. Sci.*, 1974, **18**, 963.
- Jo, W. H., Park, C. D. and Lee, M. S., *Polymer*, 1996, **37**, 1709.
- Maréchal, Ph., Legras, R. and Deconinck, J. M., *J. Polym. Sci.: Part A: Polym. Chem.*, 1993, **31**, 2057.
- Song, J., Fischer, H. and Schnabel, W., *Polymer Degradation and Stability*, 1992, **36**, 261.
- Lu, M., Keskkula, H. and Paul, D. R., *Polymer*, 1993, **34**, 1874.
- Bhowmick, A. K., Chiba, T. and Inoue, T., *J. Appl. Polym. Sci.*, 1993, **50**, 2055.
- Park, C. D., Jo, W. H. and Lee, M. S., *Polymer*, 1996, **37**, 3055.
- Dompas, D. and Groeninckx, G., *Electron Microscopy for Polymers*, EUPOCO-course, KU Leuven, Belgium, 1993–94.
- Takeda, Y. and Paul, D. R., *J. Polym. Sci.: Part B: Polym. Phys.*, 1992, **30**, 1273.
- Fortelny, I., Cerna, Z., Binho, J. and Kovar, J., *J. Appl. Polym. Sci.*, 1993, **48**, 1731.
- Fortelny, I. and Zivny, A., *Polymer*, 1995, **36**, 4113.
- Meijer, H. E. H., Lemstra, P. J. and Elemans, P. H. M., *Makromol. Chem., Makromol. Symp.*, 1988, **16**, 11.
- White, J. L. and Kim, K., *Makromol. Chem., Makromol. Symp.*, 1988, **16**, 19.
- Favis, B. D., *Polymer*, 1994, **35**, 1552.
- Sandaraj, U. and Macosko, C., *Macromolecules*, 1995, **28**, 2647.
- Favis, B. D. and Willis, J. M., *J. Polym. Sci.: Part B: Polym. Phys.*, 1990, **28**, 2259.
- Elmendorp, J. J., Ph.D. Thesis, TU Delft, 1986.
- Majumdar, B., Keskkula, H. and Paul, D. R., *Polymer*, 1994, **35**, 1386.
- Paul, D. R. and Barlow, J. W., *Polymer*, 1984, **25**, 487.
- Brannock, G. R., Barlow, J. W. and Paul, D. R., *J. Polym. Sci.: Part B: Polym. Phys.*, 1991, **29**, 413.
- Dompas, D., Groeninckx, G., Isogawa, M., Hasegawa, T. and Kadokura, M., *Polymer*, 1997, **38**, 421.
- Brochard, F., Jouffroy, J. and Levinson, P., *Macromolecules*, 1983, **16**, 1638.
- Majumdar, B., Keskkula, H., Paul, D. R. and Harvey, N. G., *Polymer*, 1994, **35**, 4263.
- Majumdar, B., Keskkula, H. and Paul, D. R., *Polymer*, 1994, **35**, 3164.
- Vanham, R., Degée, P., Jérôme, R. and Teyssié, Ph., *Polymer Bulletin*, 1994, **33**, 221.
- Kim, B. K. and Park, J. J., *J. Appl. Polym. Sci.*, 1991, **43**, 357.
- Nie, L. and Narayan, R., *Polymer*, 1994, **35**, 4334.
- Dedecker, K., Groeninckx, G., *Polymer*, 1998, **39**, 4993.
- Dedecker, K., Groeninckx, G. and Inoue, T., *Polymer*, 1998, **39**, 5001.